

Numerical simulation of a turbulent flow over a heated wall

Daniel Vieira Soares

Universidade de Brasília – Departamento de Engenharia Mecânica – 70910-900 – Brasília - DF
danielvsoares@hotmail.com

Regis Silvestre da Costa Ataídes

Empresa Brasileira de Aeronáutica S.A. - São José dos Campos – 12227-901 - SP
regis.ataides@embraer.com.br

José Luiz Alves da Fontoura Rodrigues

Universidade de Brasília – Departamento de Engenharia Mecânica – 70910-900 – Brasília - DF
fontoura@unb.br

Abstract. *The main goal of this work is to present the results of a numerical simulation of a thermal turbulent boundary layer flow, developed over a strongly heated flat plate. The algorithm used adopts the Favre averaging, equations of state for density and for molecular viscosity, the turbulence model is the classical $k-\epsilon$ of Jones and Launder (1972). The inner layer is modelled by velocity and temperature wall laws. Spatial discretization is done by P1/isoP2 finite element method and temporal discretization is implemented using a semi-implicit sequential scheme of finite difference. The coupling pressure-velocity is numerically solved by a variation of Uzawa's algorithm. To filter the numerical noises, originated by the symmetric treatment used by Galerkin method to the convective fluxes, it is adopted the balancing dissipation method proposed by Huges and Brooks (1979) and Kelly et al (1980). The remaining non-linearities, due to laws of wall, are treated by minimal residual method proposed by Fontoura Rodrigues (1991). The results were compared with the experimental data of Ng (1981) and with the numerical results obtained by one commercial solver (CFX-5.5.1). The Reynolds number of the flow, based on the outlet channel height is 66460 and the temperature of the wall was set to 1250K. The comparison was done by taking velocity and density profiles, velocity and thermal boundary layer thickness and local Stanton number along the wall. Results from the simulation with the proposed methodology were comparatively closer to experimental data than those obtained with CFX-5.5.1.*

Keywords. *turbulence, dilatable flow, Favre averaging, wall laws, finite elements.*

1. Introduction

The conferences AFORS-HTTM about complex turbulent flows, in the years 1980 and 1981 at Stanford, from which resulted the proposition of using the flow over a backward facing step as a standard case to provide analysis of numerical simulation of turbulence and respective models, are important historical marks of the studies of parietal turbulence in industry applications. Since then, the main problems encountered are still linked to representing the flow that occurs in the inner region of the boundary layer, where the intensity of local gradients and the conjugate effects of molecular viscosity and turbulent diffusivity of momentum are very difficult to be treated simultaneously.

The intensity of the gradients has as main consequence the need of very fine calculation meshes for an efficient numerical modeling of the flow in this region. The simultaneous performance of viscous and turbulent effects makes unfeasible the employment of turbulence models consecrated by the use, as the $\kappa-\epsilon$ model of Jones and Launder (1972), in the inner region of the boundary layer. As solution for these special characteristics of parietal turbulence two options exist: the use of wall laws, capable to represent the dynamic behavior of the inner region of the boundary layer, associated to conventional turbulent models and the use of special turbulence models, usually called "low Reynolds models", having each one of these solutions advantages and disadvantages.

The low-Reynolds models have two relevant inconveniences: they don't eliminate the need of very refined meshes in the immediate proximity of the walls and they are, in general, models with a small generality degree, because the simultaneous representation of the viscous and turbulent effects of the inner region of the boundary layer is done by functions set for specific geometries and specific flow conditions.

The use of laws of the wall, deduced from the governing equations of the boundary layer, associated or not with dimensional or scaling analysis, substantially reduce the need of very refined meshes in the near wall region. The greatest inconvenience of the wall laws is the numeric instability induced in the numeric algorithms that make use of this method. The flow modeling in the proximity of solid contours of the calculation domain, through wall laws, introduces a supplemental non-linear behavior the system of equations, caused by the explicit treatment that calculates the boundary conditions for the equations of the turbulence model in a given iteration, based on the previous iteration results for the velocity field, generating this way the characteristic numerical instability of the explicit iterative schemes.

In the applications that adopt procedures of temporal integration of the governing equations, which start with a random set of initial conditions and converge to a permanent situation of the flow, the instability associated to the use of wall laws is amplified, demanding the adoption of special algorithms of numeric stabilization specifically designed for this function.

In a great variety of engineering applications, the turbulent flows are used as means of transportation of thermal energy. In these circumstances, the study of the simultaneous existence, of the velocity boundary layer and the temperature boundary layer, becomes essential for the numerical modeling of the flow. The consequences of the introduction of a new dependent variable, the temperature, in the simulation of the parietal turbulence can be

summarized enumerating the needs created by this inclusion: to add to the turbulent governing equations, the mean energy equation; to select a convenient model for the correlation tensor among fluctuations of velocity and temperature; to correctly evaluate the variations of thermodynamic properties caused by the temperature variation, specifically the variations of density and molecular viscosity; to include to the algorithm temperature laws of the wall chosen to be implemented.

With all these considerations, the objective of this work is to test the numerical performance of an algorithm for the simulation of parietal dilatable turbulent flows, which happen when the turbulent flow has variations of density caused by temperature gradients, originated in the solid walls of the calculation domain.

The algorithm to be tested, Turbo 2D, is a combination of the numerical simulation methodology using finite elements of strongly heated wall flows, proposed by Brun (1988), with an error minimization method, adapted to finite elements, for the simulation of turbulent wall flows with non-linear boundary conditions, proposed by Fontoura Rodrigues (1990) e (1991).

By applying Galerkin's method for finite elements to the calculation of convection dominant flows, numerical oscillations without physical meaning can appear. This fact occurs due to the symmetric treatment given by Galerkin's method to a parabolic physic phenomenon, in accordance with Huges and Brooks (1979), which is not symmetric, in this case the convection. To lower the tendency of numerical oscillation, a balancing dissipation method, proposed by Huges and Brooks (1979) and Kelly et al. (1980) and implemented by Brun (1988), is used in Turbo 2D to prevent this occurrence.

For that, the selected test case was the heated wall flow by Ng (1981), consisting of a fully developed turbulent air flow over a wall, with 250 mm of length, heated to 1250 K. The results obtained with the above methodology are compared with experimental data of Ng (1981) and with numerical results provided by the commercial code CFX 5.5.1 from AEA Technology, adopting two different turbulent models: the classic κ - ϵ model by Jones and Launder (1972), with the improvements of Launder and Spalding (1974), using the classic logarithmic wall law and the SST model by Menter (1993), which is an improvement to Wilcox's (1998) κ - ω model, integrated until the wall of the domain.

2. Governing equations

The flow analyzed in the present work is homogeneous, one-phase, at low Mach number, and field forces are not significant. This way, the conservation equations of mass, momentum and energy, which describe the phenomenon, are represented with the relations:

$$\frac{\partial \mathbf{r}}{\partial t} + \nabla \cdot (\mathbf{r}\vec{u}) = 0, \quad (1)$$

$$\frac{\partial (\mathbf{r}\vec{u})}{\partial t} + \nabla \cdot (\mathbf{r}\vec{u} * \vec{u}) = -\nabla p + \nabla \cdot \vec{\mathbf{t}}, \quad (2)$$

$$\mathbf{r}C_p \left(\frac{\partial T}{\partial t} + \vec{u} \cdot \nabla T \right) = \frac{\partial p}{\partial t} + \vec{u} \cdot \nabla p + \nabla \cdot (k \nabla T) + \vec{\mathbf{t}} \cdot \nabla \vec{u}, \quad (3)$$

where ρ is the fluid density, t represents time, \vec{u} is the velocity field, p is the total pressure, C_p represents the specific heat coefficient at constant pressure, considered constant with temperature in the present work, T is the temperature, k is the thermal conductivity and \mathbf{t} is the shear stress tensor, with its constitutive relation for a newtonian fluid given by:

$$\vec{\mathbf{t}} = -\frac{2}{3} \mathbf{m} \nabla \cdot \vec{u} \mathbf{I} + \mathbf{m} \left[\nabla \vec{u} + \left(\nabla \vec{u} \right)^T \right]. \quad (4)$$

In relation (4), μ represents the fluid dynamic viscosity, and in this work, it is considered to be independent of the pressure, being a function of temperature only, with the relation:

$$\mathbf{m} = aT^n, \quad (5)$$

where a and n are material constants, respectively $3,68 \times 10^{-7}$ and 0,685 for the air. In order to complete the system of equations, the perfect gas relation is considered, given by:

$$\frac{p}{\mathbf{r}} = RT, \quad (6)$$

where R is a constant for the air.

2.1 Dimensionless governing equations

The process of transforming the governing equations, equations (1), (2), (3) and (6) into a dimensionless form is conventional, except the treatment given to the pressure terms, with an initial decomposition defined by:

$$p(\vec{x}, t) = p_m(t) + p_f(\vec{x}, t), \quad (7)$$

where p_m is an instantaneous mean value of the pressure field and p_f is a variation, relative to the mean value, function of time and position. This procedure allows a separate consideration of variations of pressure, given by the fluid dynamics and by thermal variations. The dynamic pressure component, p_d , and the thermodynamic pressure, p_t , are turned into a dimensionless form as below:

$$p_d = \frac{p - p_m}{\rho_0 U_0^2}, \quad (8)$$

$$p_t = \frac{p}{p_0}. \quad (9)$$

In relations (8) e (9) the sub-indexes zero characterize, respectively, the reference values for density, velocity and pressure. The relation between the dynamic component and the thermodynamic component is given by:

$$p_t = M_a^2 \gamma p_d + \frac{p_m}{p_0}, \quad (10)$$

where γ is the relation between the specific heat coefficients, at constant pressure and volume, and M_a is the Mach number, defined as a function of reference values of velocity and temperature, adopted when turning equations (1), (2), (3) e (6) into a dimensionless form.

For the final representation of the dimensionless governing equations, two simplification hypotheses are taken, considering a low Mach number in the flow considered for this work:

- the viscous dissipation term of the energy equation, equation (3), can be neglected as indicated by the results of Fulachier (1972);
- the thermodynamic pressure is reduced to a function of time only, as the first term of the second member of equation (10) tends to small values.

As a consequence, the system of equations, in dimensionless form, is given in the form:

$$\frac{\partial \mathbf{r}}{\partial t} + \nabla \cdot (\mathbf{r} \mathbf{u}) = 0, \quad (11)$$

$$\frac{\partial (\mathbf{r} \mathbf{u})}{\partial t} + \nabla \cdot (\mathbf{r} \mathbf{u} \mathbf{u}) = -\nabla p - \frac{2}{3Re} \nabla (\nabla \cdot \mathbf{u}) + \frac{1}{Re} \nabla \cdot \left[\nabla \mathbf{u} + \left(\nabla \mathbf{u} \right)^T \right], \quad (12)$$

$$\mathbf{r} \left(\frac{\partial T}{\partial t} + \mathbf{u} \cdot \nabla T \right) = \frac{1}{Re \cdot Pr} \nabla \cdot (\nabla T), \quad (13)$$

$$\mathbf{r}(T + 1) = 1. \quad (14)$$

In order to simplify the notation adopted, the variables in their dimensionless form have the same representation as the dimensional variables. The Reynolds and Prandtl Numbers, represented by Re and Pr respectively, are defined with the reference values adopted in this process.

2.2 The turbulence model

As long as computational power today is not capable of representing all turbulent scales of the flow, the methodology adopted is a transformation of the system of instantaneous dimensionless governing equations, relations (11), (12), (13), (14), into a system of mean equations, obtained using a statistical treatment in the above equations.

In cases where the flow does not show significant variations on density, the Reynolds averaging is used. But when the variations in density are significant, the Reynolds averaging becomes inconvenient, due to the high number of unknown correlations resulted, leaving the closure problem of the system of governing equations without solution.

The solution given by Favre (1965), for flows with considerable variation of density, uses the Reynolds averaging only for density and pressure, while for velocity and temperature, a mass-weighted averaging is adopted, called the Favre averaging (1965).

The closure of the mean equations is based on the hypothesis of eddy viscosity, work of Boussinesq (1877), adapted to variable density flows, by Jones and McGuirk (1979). For the velocity fluctuation correlation tensor, called Reynolds Stress, the closure takes the form:

$$\overline{\mathbf{r} \tilde{u} \tilde{u}^*} = \frac{2}{3} \left(\overline{\mathbf{r} \mathbf{k}} + \mathbf{m} \nabla \cdot \tilde{\mathbf{u}} \right) \mathbf{I} - \mathbf{m} \left[\left(\nabla \tilde{\mathbf{u}} \right) + \left(\nabla \tilde{\mathbf{u}} \right)^T \right], \quad (15)$$

where \mathbf{m} is the eddy viscosity, \mathbf{k} is the turbulence kinetic energy, and \mathbf{I} is the identity tensor. For the velocity and temperature fluctuations correlation tensor, interpreted as the turbulent flux of temperature, the proposed closure takes the form:

$$\overline{\mathbf{r} \tilde{u} \tilde{T}} = - \frac{\mathbf{m}}{\text{Pr}_t} \nabla T, \quad (16)$$

where Pr_t is the turbulent Prandtl number, considered as a constant. In order to equations (15) and (16) turn possible to solve the closure problem of the system of mean equations, it is necessary to determine the value of the eddy viscosity \mathbf{m} . The form adopted in this work to express the eddy viscosity \mathbf{m} as a function of the turbulence kinetic energy \mathbf{k} and the dissipation rate of turbulence kinetic energy \mathbf{e} , is using the Prandtl – Kolmogorov relation:

$$\mathbf{m} = C_m \mathbf{r} \frac{\mathbf{k}^2}{\mathbf{e}}, \quad (17)$$

where C_m is a constant of value 0,09. With the adoption of relation (17), the κ - ϵ turbulence model relation imposes the necessity of two supplementary transport equations to the system of mean equations, destined to evaluation of variables \mathbf{k} and \mathbf{e} .

Once defined the closure of the system of mean equations, the direction proposed by Brun (1988) produces, as a system of governing equations to density variable flows, the following system of equations:

$$\frac{\partial \overline{\mathbf{r}}}{\partial t} + \nabla \cdot \overline{\mathbf{Q}} = 0, \quad (18)$$

$$\frac{\partial \overline{\mathbf{Q}}}{\partial t} + \nabla \cdot \left(\frac{\overline{\mathbf{Q}}}{\mathbf{r}} * \overline{\mathbf{Q}} \right) = - \overline{\nabla p^*} + \nabla \cdot \left[\left(\frac{1}{\text{Re}} + \frac{1}{\text{Re}_t} \right) \left[\nabla \frac{\overline{\mathbf{Q}}}{\mathbf{r}} + \left(\nabla \frac{\overline{\mathbf{Q}}}{\mathbf{r}} \right)^T \right] \right], \quad (19)$$

$$\frac{\partial \overline{\tilde{T}}}{\partial t} + \frac{\overline{\mathbf{Q}}}{\mathbf{r}} \nabla \tilde{T} = \frac{1}{\mathbf{r}} \nabla \cdot \left[\left(\frac{1}{\text{Re} \cdot \text{Pr}} + \frac{1}{\text{Re}_t \cdot \text{Pr}_t} \right) \nabla \tilde{T} \right], \quad (20)$$

$$\frac{\partial \overline{\mathbf{k}}}{\partial t} + \frac{\overline{\mathbf{Q}}}{\mathbf{r}} \nabla \mathbf{k} = \frac{1}{\mathbf{r}} \nabla \cdot \left[\left(\frac{1}{\text{Re}} + \frac{1}{\text{Re}_t \cdot \mathbf{s}_k} \right) \nabla \mathbf{k} \right] + \Pi - \mathbf{e}, \quad (21)$$

$$\frac{\partial \overline{\mathbf{e}}}{\partial t} + \frac{\overline{\mathbf{Q}}}{\mathbf{r}} \nabla \mathbf{e} = \frac{1}{\mathbf{r}} \nabla \cdot \left[\left(\frac{1}{\text{Re}} + \frac{1}{\text{Re}_t \cdot \mathbf{s}_e} \right) \nabla \mathbf{e} \right] + C_{e1} \frac{\mathbf{e}}{\mathbf{k}} \Pi - C_{e2} \frac{\mathbf{e}^2}{\mathbf{k}}, \quad (22)$$

$$\overline{\mathbf{r}} = \frac{1}{1 + \tilde{T}}, \quad (23)$$

where

$$\bar{Q} = \bar{\mathbf{r}} \tilde{u}, \quad (24)$$

$$\frac{1}{\text{Re}_t} = C_m \bar{\mathbf{r}} \frac{\mathbf{k}^2}{\mathbf{e}}, \quad (25)$$

$$\Pi = \frac{1}{\bar{\mathbf{r}}} \left[\frac{1}{R_t} \left[\nabla \frac{\bar{Q}}{\bar{\mathbf{r}}} + \left(\nabla \frac{\bar{Q}}{\bar{\mathbf{r}}} \right)^T \right] - \frac{2}{3} \left(\bar{\mathbf{r}} \mathbf{k} + \frac{1}{\text{Re}_t} \nabla \cdot \frac{\bar{Q}}{\bar{\mathbf{r}}} \right) \bar{\mathbf{I}} \right] \nabla \frac{\bar{Q}}{\bar{\mathbf{r}}}, \quad (26)$$

$$\overline{\nabla p^*} = \bar{p} + \frac{2}{3} \left[\left(\frac{1}{\text{Re}} + \frac{1}{\text{Re}_t} \right) \nabla \cdot \frac{\bar{Q}}{\bar{\mathbf{r}}} + \bar{\mathbf{r}} \mathbf{k} \right]. \quad (27)$$

The calibration constants of the model are:

$$C_m = 0.09, \quad C_{e1} = 1.44, \quad C_{e2} = 1.92, \quad \mathbf{s}_k = 1, \quad \mathbf{s}_e = 1.3, \quad \text{Pr}_t = 1.5.$$

2.3 Near wall treatment

The κ - ϵ turbulence model is incapable of properly representing the laminar sub-layer and the transition regions of the turbulent boundary layer. To solve this inconvenience, the solution adopted in this work is the use of wall laws for temperature and for velocity, capable of properly representing the flow in the inner region of the turbulent boundary layer. For the velocity calculation, the solution employed is the classical wall law logarithmic formulation, which is well known and further explanation is unnecessary.

For the calculation of the temperature, a friction temperature T_F is defined as:

$$T_F u_F = \left[\frac{1}{\text{Re Pr}} \frac{\partial \tilde{T}}{\partial n} - u'' \tilde{T}'' \right]_y = \left[\left(\frac{1}{\text{Re Pr}} + \frac{1}{\text{Re}_t \text{Pr}_t} \right) \frac{\partial \tilde{T}}{\partial n} \right]_y, \quad (28)$$

where n represents the normal direction to the wall. The friction velocity u_F is defined as

$$u_F = \sqrt{\frac{\mathbf{t}_p}{\bar{\mathbf{r}}}} \quad \text{with} \quad y^+ = \frac{u_F y}{\mathbf{n}}. \quad (29)$$

The wall laws adopted in this work for the viscous sub-layer and the logarithmic region, proposed by Cheng and Ng (1982), are respectively:

$$\frac{(T_p - \tilde{T})_y}{T_F} = y^+ \text{Pr} \quad \text{if} \quad y^+ \leq 15.96, \quad (30)$$

$$\frac{(T_p - \tilde{T})_y}{T_F} = \frac{1}{K'} \ln y^+ + C' \quad \text{if} \quad y^+ > 15.96, \quad (31)$$

where T_p represents the temperature on the wall, K' and C' are constants set experimentally by Cheng and Ng (1982) respectively equal to 0,8 and 12,5. For numerical implementation, the separation point between the viscous sub-layer and the logarithmic region of the turbulent thermal boundary layer is 15.96.

In the inner region of the turbulent boundary layer, the transport equations for turbulence kinetic energy and its dissipation rate are reduced to the equilibrium of production and dissipation.

3. Numerical methodology

The numerical solution of the proposed system of governing equations, of a dilatable turbulent flow, has as main difficulties: the coupling between all equations; the non-linear behavior resulting of the simultaneous action of convective and eddy viscosity terms; the explicit calculations of boundary conditions in the solid boundary; the methodology of use the continuity equation as a manner to link the coupling fields of velocity and pressure.

The solution proposed in the present work suggests a temporal discretization of the system of governing equations with a sequential semi-implicit finite difference algorithm proposed by Brun (1988) and a spatial discretization using finite elements of the type P1-isoP2.

3.1 Temporal discretization

The system of governing equations is spatially discretized using a first order approximation to the temporal derivative, obtained with a sequential semi-implicit finite difference algorithm, with first order truncating error, which allows a complete linearization of all equations at each time step. The algorithm proposed by Brun (1988) starts the calculation with a known field at an instant $n\Delta t$, calculating the momentum, the pressure, the temperature, the density, the turbulence kinetic energy and its dissipation rate at an instant $(n+1)\Delta t$, where n is a integer number and Δt is a time interval, by means of a sequence of calculations divided in four stages. On the first stage, the temperature field at an instant $(n+1)\Delta t$ is obtained using the relation:

$$\frac{\tilde{T}^{n+1} - \tilde{T}^n}{\Delta t} + \tilde{u}^n \cdot \nabla \tilde{T}^{n+1} = \frac{1}{\tilde{r}^n} \nabla \cdot \left[\left(\frac{1}{\text{Re Pr}} + \frac{1}{\text{Re}_t^n \text{Pr}_t} \right) \nabla \tilde{T}^{n+1} \right]. \quad (32)$$

On the second stage, the density is obtained at an instant $(n+1)\Delta t$, with the equation of state:

$$\tilde{r}^{n+1} = \frac{1}{\tilde{T}^{n+1}}. \quad (33)$$

On the third stage, the fields of momentum and pressure are calculated at instant $(n+1)\Delta t$, using a variation of Uzawa's minimum residuals algorithm proposed by Buffat (1981), with the coupled system of equations:

$$\frac{\tilde{r}^{n+1} - \tilde{r}^n}{\Delta t} + \nabla \cdot \vec{Q}^{n+1} = 0, \quad (34)$$

$$\frac{\vec{Q}^{n+1} - \vec{Q}^n}{\Delta t} + \nabla \cdot \left(\tilde{u}^n * \vec{Q}^{n+1} \right) = -\nabla \tilde{p}^{*n+1} + \nabla \cdot \left\{ \left(\frac{1}{\text{Re}} + \frac{1}{\text{Re}_t^n} \right) \left[\left(\frac{\vec{\nabla} \vec{Q}^{n+1}}{\tilde{r}^{n+1}} \right) + \left(\vec{\nabla} \tilde{u}^n \right)^T \right] \right\}. \quad (35)$$

On the fourth and last stage, all other values are calculated at instant $(n+1)\Delta t$:

$$\frac{\mathbf{k}^{n+1} - \mathbf{k}^n}{\Delta t} + \tilde{u}^n \cdot \nabla \mathbf{k}^{n+1} = \frac{1}{\tilde{r}^{n+1}} \nabla \cdot \left[\left(\frac{1}{\text{Re}} + \frac{1}{\text{Re}_t^n \mathbf{S}_k} \right) \nabla \mathbf{k}^{n+1} \right] + \Pi^{n+1} - \frac{\mathbf{e}^n}{\mathbf{k}^n} \mathbf{k}^{n+1}, \quad (36)$$

$$\frac{\mathbf{e}^{n+1} - \mathbf{e}^n}{\Delta t} + \tilde{u}^n \cdot \nabla \mathbf{e}^{n+1} = \frac{1}{\tilde{r}^{n+1}} \nabla \cdot \left[\left(\frac{1}{\text{Re}} + \frac{1}{\text{Re}_t^n \mathbf{S}_e} \right) \nabla \mathbf{e}^{n+1} \right] + C_{e1} \frac{\mathbf{e}^n}{\mathbf{k}^n} \Pi^{n+1} - C_{e2} \frac{\mathbf{e}^n}{\mathbf{k}^n} \mathbf{e}^{n+1}, \quad (37)$$

with the following expression for the production term:

$$\Pi^{n+1} = \frac{1}{\tilde{r}^{n+1}} \left[\frac{1}{\tilde{R}_t^n} \left[\vec{\nabla} \tilde{u}^{n+1} + \left(\vec{\nabla} \tilde{u}^{n+1} \right)^T \right] - \frac{2}{3} \left(\tilde{r}^n \mathbf{k}^n + \frac{1}{\text{Re}_t^n} \nabla \cdot \tilde{u}^{n+1} \right) \tilde{I} \right] \vec{\nabla} \tilde{u}^{n+1}, \quad (38)$$

and finally, the following values are updated:

$$\frac{1}{\text{Re}_t^{n+1}} = C_m \bar{\mathbf{r}}^{n+1} \frac{(\mathbf{k}^{n+1})^2}{\mathbf{e}^{n+1}}, \quad (39)$$

$$\bar{\mathbf{u}}^{n+1} = \frac{\bar{Q}^{n+1}}{\bar{\mathbf{r}}^{n+1}}. \quad (40)$$

As the boundary conditions are calculated explicitly, based on values of the instant $n\Delta t$ to determine the conditions for the instant $(n+1)\Delta t$, a numerical instability inevitably appears. To eliminate this characteristic of the use of wall laws, in applications where temporal variations are considered, the minimization residuals technique proposed by Fontoura Rodrigues (1991), that adopts an iterative calculation sequence based on the minimization of the resulting error on the evaluation of the friction velocity, defined for a determined iteration i at an instant $(n+1)\Delta t$, as:

$$(\text{Error})_i^{n+1} = \left\| (u_F^2)^* - (u_F^2)_i^{n+1} \right\|, \quad (41)$$

where the double bars indicate the absolute values of the vectors, the value of $(u_F^2)^*$ is obtained with the wall laws relation, with values of iteration i at instant $(n+1)\Delta t$, and the value of $(u_F^2)_i^{n+1}$ is obtained with a numerical relation of recurrence, from the error minimization algorithm.

3.2 Spatial discretization

The system of governing equations is discretized in space using triangular finite elements, defined by linear interpolation functions. The compatibility conditions between pressure and velocity is preserved using two calculation meshes. The pressure field is calculated with a mesh with elements of types P1. The velocity and all other variables are calculated using a P1-isoP2 mesh, defined from the P1 mesh by dividing one segment into two, this way, generating four P1-isoP2 elements from one P1 element. Figure (1) shows the velocity and pressure meshes used to calculate the flow studied in this work.

4. Numerical results

The methodology for simulating the thermal boundary layer, presented in this work, was tested with a fully developed air flow simulation, which goes over a heavily heated horizontal wall. The basis for the validation of the results is the experimental data of Ng (1981).

The test case of Ng (1981), the flow is totally developed in a wind tunnel, with temperature of 293 K and free flow velocity of 10,7 m/s. This flow passes through the test area, the horizontal plate with 250 mm of length, kept at constant temperature of 1250 K. The final part of the development of the velocity profile is done in a channel of square section with 100 mm of edge and 500 mm of length. At beginning of the channel, measuring 250 mm of length, a rough cover was placed on the inferior wall in order to accelerate the development of the flow. On the second half of the channel, the inferior wall is flat, made of identical materials and superficial finish to the test section, which is a natural prolongation of the inferior wall of the channel, totally exposed to the atmosphere of the laboratory. The Reynolds number of the flow, taking the length of the edge normal to the test section as a characteristic length, is 66460.

The adopted calculation domain is correspondent to the test section only, constituted by a rectangle measuring 50 mm of height and 250 mm of length, calculating the area affected by the presence of the wall only, the upper part of the test section is not influenced by the wall, having as fields the reference values of the variables, causing no influence on the numerical simulation. Figure (1) shows the meshes for pressure and velocity calculations. The code Turbo2D, responsible for the implementation of the proposed methodology in the present work, makes use of both pressure and velocity meshes shown in figures (1a) and (1b) respectively. The code CFX, used to compare the numerical results, makes all calculations with the velocity mesh only, shown in figure (1b).

The boundary conditions for the three simulations were:

- for the inlet of the calculation domain, the experimental profiles provided by the work of Ng (1981) were imposed for temperature, velocity, turbulence kinetic energy and its dissipation rate;
- for the heated wall, the code Turbo2D uses wall laws, for velocity and for temperature, set for a value of y^+ equal to 50; for the κ - ϵ model, the code CFX 5.5.1, which also works with wall laws, the value of y^+ is limited to 11, for the SST model, the code CFX 5.5.1 integrates the equations to the wall, with boundary condition of impermeability and temperature of 1250 K;
- for the upper part of the domain, the area of free flow, pressure and temperature are set to ambient values of the laboratory, and for the components of u , κ and ϵ the same values of the experimental profiles of the inlet of the domain were adopted, and for the vertical component of the momentum, null derivative were imposed;
- for the region of the outlet of the domain, the relative pressure is set to zero and all other variables are set to have null derivative for the normal direction to the flow.

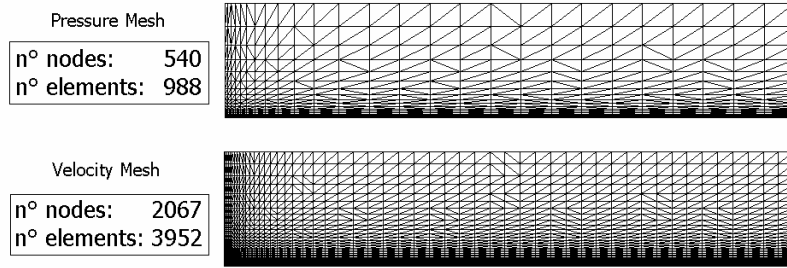


Figure 1: Pressure mesh (a) and velocity mesh (b) with respective numbers of nodes and elements

The numerical simulation was implemented in two steps, following the experimental methodology adopted by Ng (1981) to evaluate the effects of temperature on the flow. Initially, an isothermal flow was simulated, that was used as reference for the second stage, the simulation of the flow over the strongly heated wall.

The present work has as objective to test a methodology for simulating the thermal boundary layer. The results presented are relating to the thermal boundary simulation, of the flow over the strongly heated wall, displaying profiles of velocity and density at two stations on the wall, at 125 mm and 182 mm, starting from the beginning of the test area, and results concerning the fields calculated through all the extension of the wall, represented by the velocity boundary layer thickness, the thermal boundary layer thickness and the profile of the local Stanton number along the length of the wall.

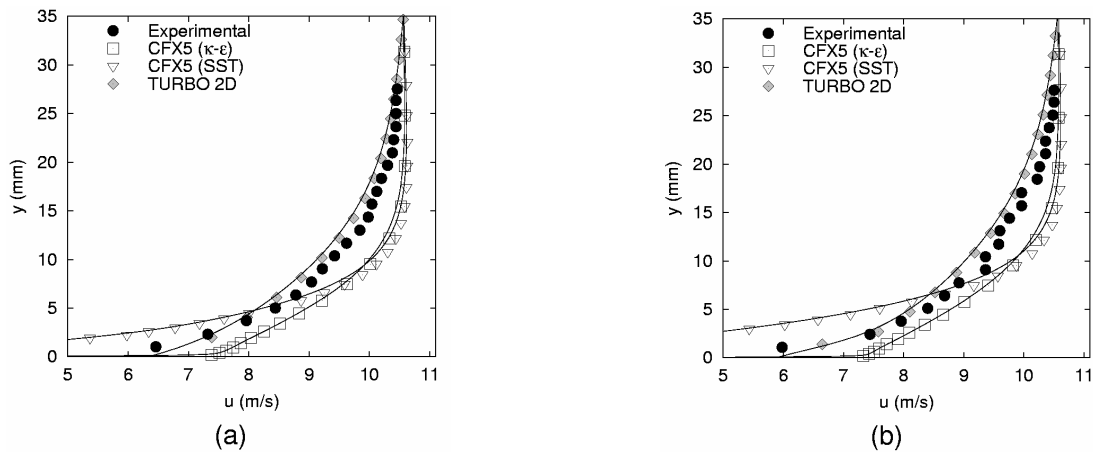


Figure 2: Velocity profiles at 125 mm (a) and at 182 mm (b)

In figures (2a) and (2b) the calculated velocity profiles are shown, respectively at 125 mm and 182 mm from the starting edge of the plate. The y axis represents the normal distance to the heated wall, in millimeters, and the x axis represents the longitudinal component of the velocity, in meters per second. The results in figure (2a) show that the profile obtained with Turbo2D is close to the experimental data along all the boundary layer, and the results obtained with CFX 5.5.1 do not have the same quality, for both SST and $\kappa\text{-}\epsilon$ models, mainly inside the inner region of the boundary layer. To the profile of figure (2b), the results are the same, not showing any significant alteration. It is possible to notice by these profiles, that the velocity boundary layer has approximately 20 mm of thickness, in this region of the heated plate.

In figures (3a) and (3b) the obtained profiles of density at stations 125 mm and 182 mm from the starting edge of the plate are shown. The y axis represents the normal distance from the wall and the x axis the density, respectively in millimeters and in kilograms per cubic meter. The results obtained show that the result obtained with CFX-5 using a $\kappa\text{-}\epsilon$ model is closer to experimental data than the other simulations. Turbo2D and CFX with SST provided very close results from each other, with little advantage of the SST model.

In figures (4a) and (4b), are shown respectively the velocity boundary layer thickness and the thermal boundary layer thickness, along the length of the heated wall. In these figures, the y axis represents the thickness of the boundary layers of velocity and temperature, in millimeters, and the x axis the position along the heated wall. The result of figure (4a) shows that the estimated thickness of all velocity boundary layer obtained with the code Turbo2D is far better than those obtained with the $\kappa\text{-}\epsilon$ and SST models of CFX 5.5.1. The simulations with the two models of CFX 5.5.1, underestimate the velocity boundary layer thickness along the length of the wall. To the thermal boundary layer, results obtained with Turbo2D and SST model of CFX 5.5.1 are very good, with better approximation to experimental data obtained with Turbo2D. The $\kappa\text{-}\epsilon$ model of CFX 5.5.1 is the worst simulation of the thermal boundary layer thickness.

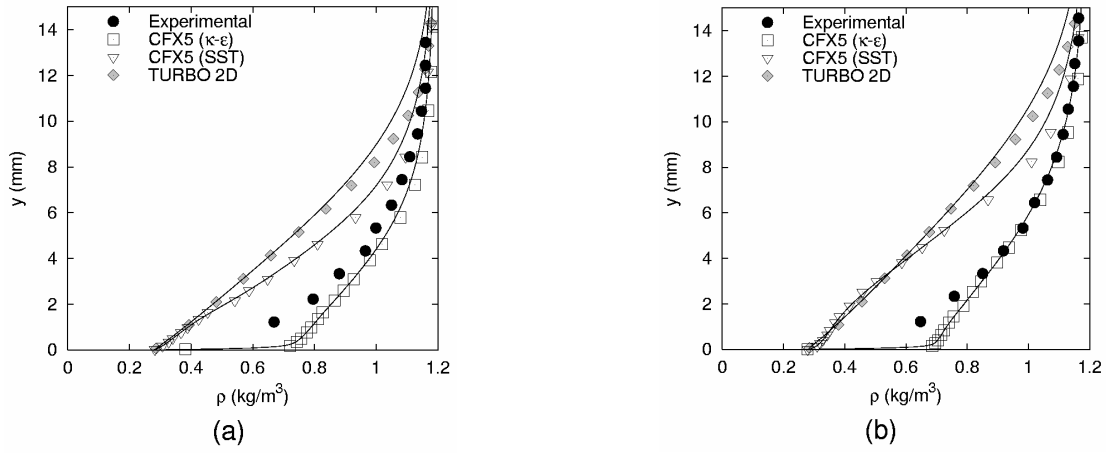


Figure 3: Density profiles at 125 mm (a) and at 182 mm (b)

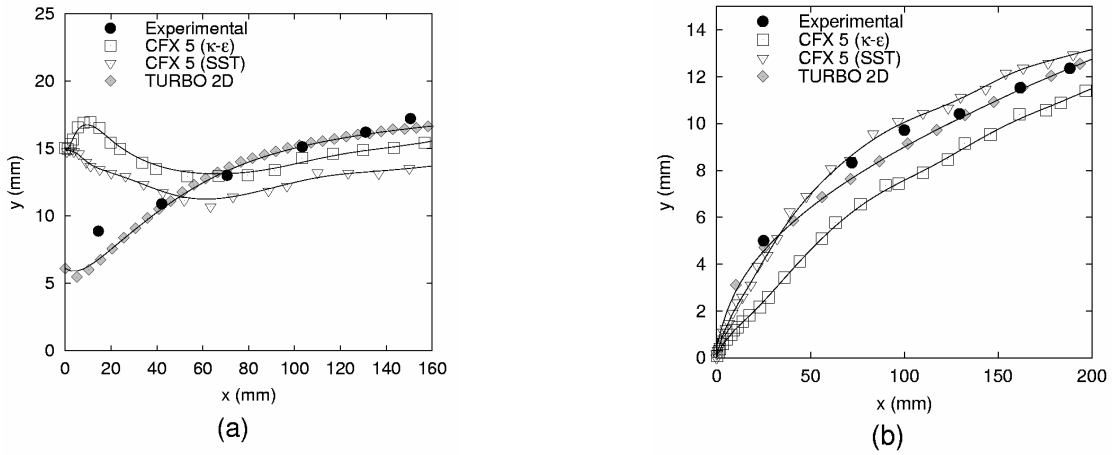


Figure 4: Velocity boundary layer thickness (a) and thermal boundary layer thickness (b) along the wall

In figure (5) is shown the corresponding local Stanton number, calculated along the length of the plate with the relation recommended by Incropera e DeWitt (1996), by relation (42), where the temperature gradient is taken its non dimensional form:

$$St_x = \frac{\left(\frac{\Delta T}{\Delta y} \right)_{y=y^+} \left(\frac{d_T}{T_w - T_\infty} \right)}{\left(\frac{u_F x}{n} \right) \left(\frac{n}{a} \right)}. \quad (42)$$

In figure (5) the y axis represents the local Stanton number and the x axis represents the length taken from the beginning of the heated plate, in millimeters. The best estimative was obtained with Turbo2D, with κ - ϵ model of CFX 5.5.1 also showing good results in accordance with the experimental data. The results obtained with SST model shows numerical oscillations with no physical meaning.

5. Conclusions

From the results obtained with the three simulation, the profiles of velocity, the velocity and thermal boundary layer thickness and local Stanton Number, it is shown that the best accordance with experimental data was obtained with the algorithm proposed in this work and implemented by Turbo2D software.

The disagreement between the results obtained with the three simulations for the density profiles, indicates that the treatment applied to the equation of state used in the simulations is critical. In the three simulations, the ideal gas model was used, but the code CFX 5.5.1 evaluates the local values of C_p as a function of the temperature, and the code Turbo2D takes a constant value of C_p .

The numerical oscillations obtained in the results of the SST model are caused by the instability of the values of friction velocity, originated because this model integrates the governing equations up to the wall and the mesh adopted for the calculation is not sufficiently refined for these operations. The oscillations obtained with the SST model could be

avoided using a more refined mesh than the one adopted for the comparison, but a greater computational effort would be needed.

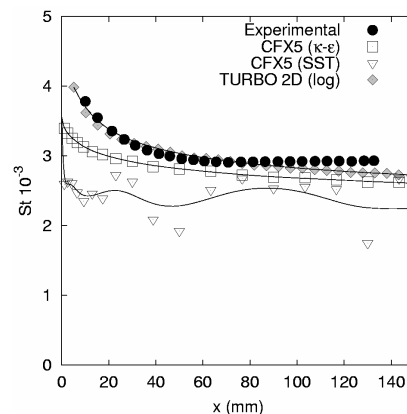


Figure 5 – Local Stanton number along the wall

6. Acknowledgments

We are grateful to the colleagues, professors and students of the Group of Complex Fluid Dynamics – Vortex, from the Department of Mechanical Engineering of University of Brasília, for the encouragement and technical support during the accomplishment of this work. We also thank the Technology and Scientific Enterprise Foundation – FINATEC, for the material and financial support, which made this work possible.

7. References

- AFOSS-HTTM, 1980-1981, “Stanford Conference on Complex Fluid Flow”, Stanford, USA.
- Boussinesq, J., 1877, “Théorie de l’Écoulement Tourbillant”, Mem. Présentés par Divers Savants Acad. Sci. Inst. Fr., vol. 23, pp. 46-50.
- Brun, G., 1988, “Developpement et application d’une methode d’elements finis pour le calcul des ecoulements turbulents fortement chauffés”, Tese de Doutorado, Laboratoire de Mécanique des Fluides, Escola Central de Lyon.
- Buffat, M., 1981, “Formulation moindre carrés adaptées au traitement des effets convectifs dans les équation de Navier-Stokes”, Doctorat thesis, Université Claude Bernard, Lyon, France.
- Cheng, R.K. & Ng, T.T., 1982, “Some aspects of strongly heated turbulent boundary layer flow”. *Physics of Fluids*, vol. 25(8).
- Favre, A., 1965, “Equations de gaz turbulents compressibles”. *Journal de mecanique*, vol. 3 e vol. 4.
- Fontoura Rodrigues, J. L. A., 1990, “Méthode de minimisation adaptée à la technique des éléments finis pour la simulation des écoulements turbulents avec conditions aux limites non linéaires de proche paroi”, Doctorat thesis, Ecole Centrale de Lyon, France.
- Fontoura Rodrigues, J. L. A., Brun G., Jeandel, D., 1991, “Um método de mínimo resíduo adaptado ao cálculo de condições de contorno não lineares no escoamento turbulento bidimensional”, XI Congresso Brasileiro de Engenharia Mecânica – COBEM, p. 465
- Fulachier, L., 1972, “Contribution à l’étude des analogies des champs dynamique et thermique dans une couche limite turbulent – effet de l’aspiration”, Thèse D’Etat – IMST, Marseille, France.
- Incropera, F.P. and DeWitt, D.P., 1996, “Fundamentos de Transferência de Calor e de Massa, 4ª Edição”, LCT Livros Técnicos e Científicos Editora S.A., São Paulo, Brasil.
- Jones, W. and Launder, B.E., 1972, “The prediction of laminarization with a two equations model of turbulence”, *International Journal of Heat and Mass Transfer*, vol. 15, pp. 301-314.
- Jones, W.P. and Mc Guirk, J.J., 1979, “Mathematical modelling of gas-turbine combustion chambers”, AGARD, p. 275
- Launder, B.E., Spalding, D.B., 1974, “The numerical computation of turbulent flows”, *Computational Methods Applied to Mechanical Engineering*, vol. 3, pp. 269-289.
- Menter, F.R., 1993, “Zonal two equation k- ω turbulence models for aerodynamic flows”, AIAA, vol. 93, pp. 2906.
- Ng, T.T., 1981., “Experimental study of a chemically reacting turbulent boundary layer”, Ph. D. Thesis, Lawrence Berkley Laboratory, University of California.
- Wilcox, D.C., 1998, “Turbulence modeling for CFD Second Edition”, DCW Industries Inc, USA.